# Experimental testing of 3DCP reinforcement Wall segments

*Vojtech* Vanek[1*], *David* Beckovsky[1], *Ondrej* Nespesný[1], *Jan* Vystrcil[1], and *Jan* Pencík[1]

[1]Faculty of Civil Engineering, Institute of Building Structures, Brno University of Technology, Veveri 331/95, 602 00 Brno, Czech Republic

**Abstract.** The wall segments are formed using additive layer-on-layer technology. The concrete mix is therefore laid in layers and the final desired element is gradually formed. The manufactured columns are all of different shapes and reinforcements. The columns are adapted for lateral load testing, whereby they are subjected to three-point bending when loaded in service. A stress of 1 MPa is transmitted to these columns and the columns are progressively loaded with a horizontal force. The test is primarily to determine how much stress these columns can carry in the wall plane in tension bending. The results of the measurements are compared with brick masonry.

## 1 Introduction

Additive manufacturing (AM), or the incremental method, was developed in the early 1980s by Charles W. Hull [1]. The main invention, called stereography, is believed to be the first incremental method using UV light. Subsequently, the knowledge of this technology was deepened, resulting in the development of new AM methods. These may be the fabrication methods called Fused Deposition Modelling (FDM) [2], Selective Laser Melting (SLM) [3]. These methods are based on the 3D printing method. AM is an incremental method, and it is not only from 3D printing as it is promoted. An example of an incremental method is Laminated Object Manufacturing (LOM) [4].

These fabrication methods have recently been joined by a method of 3D printing concrete, the Paste Extrusion Modelling (PEM) method [5]. The fabrication method is based on robotic arms, frame printers and gantry printers. The first such printers were made in 2000 [6], [7]. Print heads with nozzles are then placed on the endpoints, either active [8] or passive [9]. Most of the methods are very similar, but the fabrication of different structural elements depends on the method used. Each method contains new possibilities and research in the field.

However, this is why creating structures using additive technologies is so popular in the world. In the literature Huang S. et al. [10], forty-two structures that were produced using 3D printing are listed. Mostly, these are single-storey civil engineering buildings that are manufactured on site at the future location of the building, or these elements are manufactured by companies inside the halls as prefabricated parts, which are then transported

* Corresponding author: Vojtech.Vanek2@vutbr.cz

to the construction site where they are subsequently connected to form a perfect uniform structure. They are also used in road structures such as bridge structures, where they can be printed to support bicycle roads and bridge irregularities in the terrain [11].

In civil engineering, additive technology is most used for wall structures. Vertical load bearing structures include all wall and column structures that are at a perpendicular or partially acute or obtuse angle to the vertical tangent of the structure. 3D printed concrete structures are mostly primarily used for these vertical structural elements and structures. When comparing these 3D printed concrete vertical structures with conventional methods of construction such as small- and large-scale masonry systems using mini-cranes, timber buildings, or solid concrete structures, emphasis must be placed on speed of construction, assessment for load-bearing capacity and reliability, thermal engineering, and more.

This paper focuses on determining the maximum forces on different geometries when compared with brick masonry. These comparisons will also include different reinforcement elements and other possible reinforcement.

# 2 Material and Methods

## 2.1 Material

The test specimens were made from precast mixtures that were mixed at a ratio of 1:2. The modified mix was applied to the outer perimeter of the structure, and the material properties are shown in Table 1-2. The mixing was done to add cellulose fibres in one of the mixes. Without this combination, the structure would have been weakened and larger shrinkage cracks or even destruction of the specimen could have occurred. The inner filler was made from a prefabricated material designed for 3D printing with the properties of see Table 3.

**Table 1.** Material mechanical characteristic of one peace prefabricate mixture.

| | |
|---|---|
| Grain size | <1.0 mm |
| Flexural tensile strength after 28 days | min. 8 MPa |
| Compressive strength after 28 days | min. 40 MPa |
| Density | 2150 $kg.m^{-3}$ |

**Table 2.** Material mechanical characteristic of two peace prefabricate mixture.

| | |
|---|---|
| Grain size | <1.0 mm |
| Flexural tensile strength after 28 days | min. 6 MPa |
| Compressive strength after 28 days | min. 30 MPa |
| Density | 2000 $kg.m^{-3}$ |

**Table 3.** Material mechanical characteristic of prefabricate mixture to the infill.

| | |
|---|---|
| Grain size | <0.5 mm |
| Flexural tensile strength after 28 days | min. 7 MPa |
| Compressive strength after 28 days | min. 50 MPa |
| Density | 2000 - 2200 $kg.m^{-3}$ |

The wall structures are reinforced with concrete ladder steel. The steel is marked B500B. The steel therefore has mechanical properties in tensile strength 550 MPa and yield strength 500 MPa. The steel members will form the reinforcement baskets located inside the columns.

## 2.2 Design and Manufacturing of Segments

The design geometry is based on test blocks of brickwork. The experimental wall segments were designed with basic dimensions of 340 mm thickness, 790 mm width and 1000 mm specimen height. The width of the printed footprint was set to 45 mm, with a contact area of 30 mm according to the output passive print head. The height of the printed trace based on the flow rate and the speed of the robotic arm was set to 15 mm. One printed layer consists of one trace, i.e. a single perimeter printing method was used. The figures given are the same for all test wall segments. The proposed variants are then subdivided according to the internal reinforcement elements. These are round reinforcement columns with an internal diameter of 120 mm or square columns with internal dimensions of 110 × 110 mm. The geometry of the variant segments can be observed in Fig. 1.

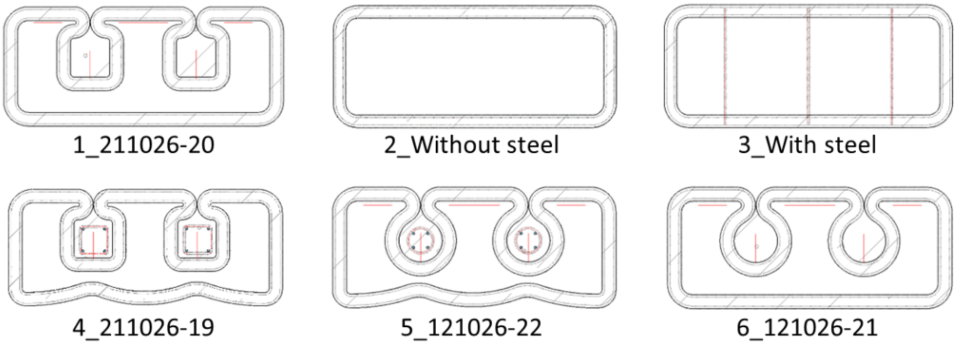


**Fig. 1.** Geometry of the 3DCP wall segments variants.

After creating the geometry in the Rhino modelling program, the modelled segments were inserted into a special program. Here the segments were divided and edited for printing. Printing was then carried out on a KUKA robotic arm. A so-called passive print head [9] was used for printing. The extrusion of the material was guided in a flexible pipe by a screw feeder, which was placed outside the robotic arm. The printing speed was set to an average of 150 mm.s$^{-1}$. The created and prepared segments were transported to the test laboratory.

Reinforcement baskets were fabricated for the internal columns using reinforcing steel with 8 mm diameter main members and 6 mm split reinforcement. The reinforcement baskets were made in two variants. The square baskets were made in the size of 85 × 85 × 1000 mm and the circular baskets were made with a diameter of 80 mm and a height of 1000 mm as can be observed in Fig. 2. Subsequently, they were inserted into the hollow reinforcement columns and were cast with precast compound after 3D printing.

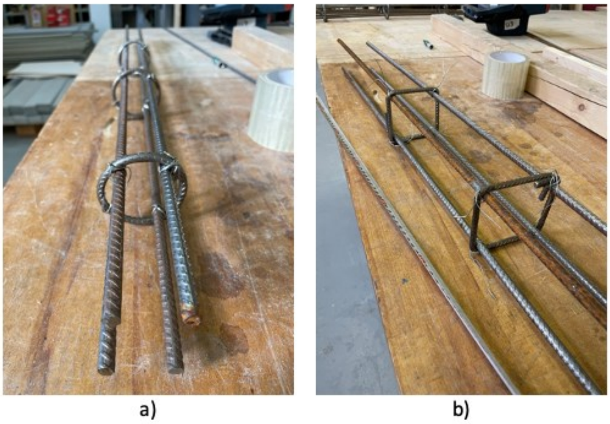


**Fig. 2.** Reinforcement cage made of concrete steel a) circle, b) square.

### 2.3 Testing Method

The test of the experimental segments was designed for three-point bending (3PB). The testing was carried out according to Czech norm ČSN 73 2030. The measurements were oriented vertically. The support points were made of I-shaped steel sections on which 50 mm wide steel washers were placed. The axial distance of the supports was set at 700 mm. The whole load assembly is shown in Fig. 3.

The loading was induced in the horizontal direction and the applied force was applied perpendicular to the wall plane. The applied force was applied by a hydraulic linear actuator SCA 65. The loading was carried out at a constant strain increment $s_l = 0.083$ mm.s$^{-1}$. The measuring range of the external pressure transducer at the end of the hydraulic actuator was 0-100 kN. Measurement of the deflection path was carried out using potentiometric cable path sensors. The transducers recorded the deflections of the experimental specimens at four points 15-18. As can be seen from Fig. 3, the sensors were located at half the distance of the supports in the pulling region and two were located above the supports in the pushing region. The potentiometers and the hydraulic press were connected to a central control panel which was connected to a PC. Eight readings were recorded for each sample during the measurement process. The sampling frequency of the control panel was set at 5 Hz.

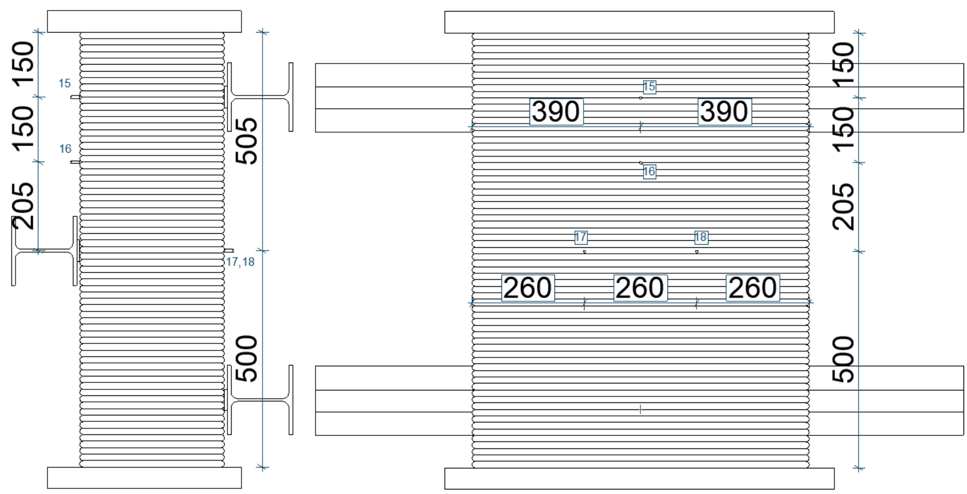


**Fig. 3.** Schematic of the 3DCP wall segment test load system.

## 3 Results and Discussion

### 3.1 Geometry of Specimens

Data evaluation was performed systematically. Input values such as height, width and length of segments were recorded before measurement. The recording of these values was done using a conventional tape measure with a preference to 1.0 mm. Since the segments are organic in shape for accuracy of measurement a 3D scanner was used. It was used to record the top printed area of the segments. The read area was then used in the calculation and determination of the force for the 1 MPa loading. Fig. 4. shows the loading scheme and the real prepared test just before the measurement.

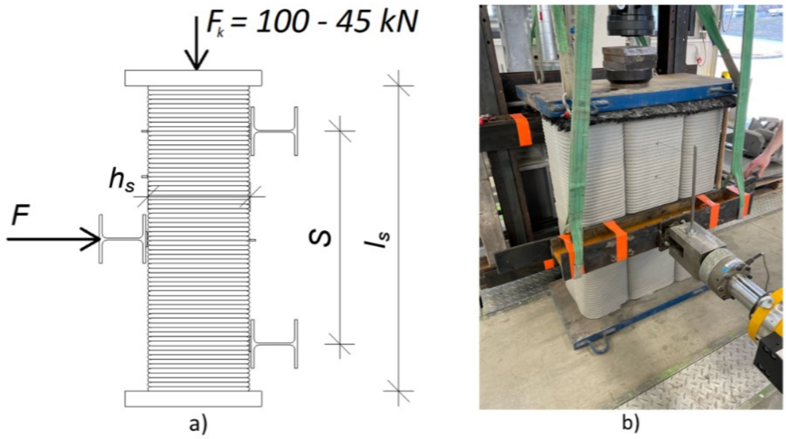


**Fig. 4.** Loading style, a) Geometry diagram; b) Real measurement; where *F* [kN] is force, $h_s$ [mm] is hight of specimen, *S* [mm] is distance of supports, $l_s$ [mm] is length of specimen and $F_k$ [kN] is force of attraction.

### 3.2 Segment Behaviour Characteristic

The results of the test were recorded in a chart. In Fig. 5, the measured data from all experimental segments are shown. The curves of each test sample are different at first glance. The diagram describes on the horizontal axis the deflection of the specimen in the middle of the span, with the measurement points 17/18. The values from the measured points 17/18 were averaged. Segment 02 and 03 have many times lower strength than segments 01,04-06. This behaviour is due to the absence of internal reinforcing columns. The graphical representation shows the different behaviour of segments 02 and 03, where it is confirmed that the internal reinforcement has an effect on the force transmitted by the stiffeners and thus the strength of the specimen itself is increased. The behaviour is confirmed by other samples. Segments 01,02,04-06 did not contain horizontal reinforcement and therefore did not have as much deflection of the segments on the drawn part as test specimen 03.

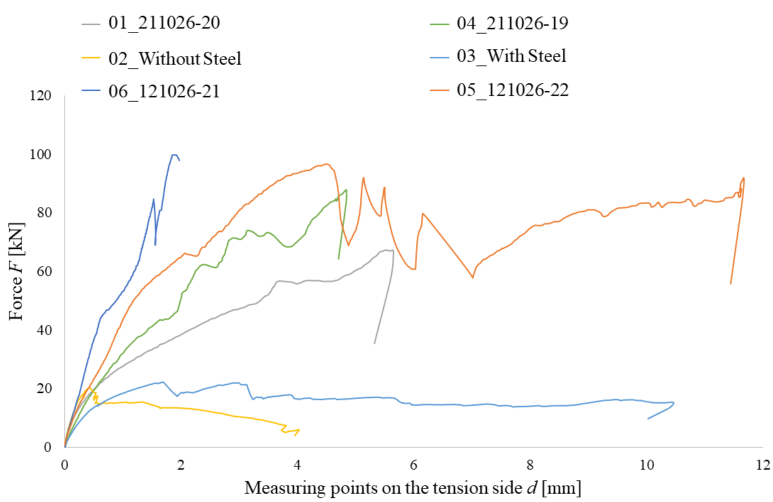


**Fig. 5.** Graphical representation of the dependence of the applied force on the deflection of the specimens. The dependence of horizontal reinforcement in the specimen is evident from test specimen 03 compared to 01,02,04-06.

The maximum achieved forces from the measurements were determined. In the initial loading condition, linear behaviour can be observed for all tested segments. The initial behaviour is linear in 80 % of the cases up to 16 kN. Subsequently, microcracks and certainly cracks are likely to occur which weaken the segments, as can be seen in Fig. 6. During further loading of the structures, stiffening elements start to appear.

a) b)

**Fig. 6.** Experimental specimens after completion of 3PB test a) without internal reinforcing columns 02/03; b) with reinforcing internal columns 01/04/05/06.

The experimental specimens labelled 2 and 3 are several times weaker in terms of strength relative to the segments with internal columns. The characteristic behaviour of these segments is in their internal reinforcement. A higher deflection can be observed for the segment with steel reinforcing bars. The maximum loads differ by a percentage difference of 10 % when comparing specimens 2 and 3.

The reinforcing bars present in segments 1,4,5,6 contribute to several times higher strength of the segments. Four times higher force absorption can be observed than in samples 2 and 3. Therefore, Table. 4 has been created, where the maximum loads achieved are presented in conjunction with the maximum deflection of the specimen on the tensile side and the force at initiation of the first cracks.

**Table 4.** Maximum and initiating forces applied to the test specimen segment.

| Lable | Max Force $F_{max}$ [kN] and Deformation $d_{max}$ [mm] | | Initiating force $F_{inc}$ [kN]: |
|---|---|---|---|
| 4_211026-19 | $F_{max}$ = | 87.88 kN | $F_{inc}$ = 73.04 kN |
| | $d_{max}$ = | 4.8367 mm | |
| 1_211026-20 | $F_{max}$ = | 67.27 kN | $F_{inc}$ = 56.64 kN |
| | $d_{max}$ = | 5.5123 mm | |
| 6_121026-21 | $F_{max}$ = | 99.75 kN | $F_{inc}$ = 45.13 kN |
| | $d_{max}$ = | 1.9143 mm | |
| 5_121026-22 | $F_{max}$ = | 96.60 kN | $F_{inc}$ = 65.71 kN |
| | $d_{max}$ = | 4.4988 mm | |
| 3_With steel | $F_{max}$ = | 22.26 kN | $F_{inc}$ = 22.26 kN |
| | $d_{max}$ = | 1.6989 mm | |
| 2_Without steel | $F_{max}$ = | 20.29 kN | $F_{inc}$ = 20.29 kN |
| | $d_{max}$ = | 0.4299 mm | |

Brick masonry was used to compare the results. The masonry achieved a characteristic flexural tensile strength at failure in the plane parallel to the bearing joints of $f_{xk} = 0.36$ N.mm $^{2}$. Percentage comparisons between the values of the brick masonry and 3DCP wall segments are shown in Table 5.

**Table 5.** Calculation and comparation of flexural tensile strength from maximum force.

| Lable | $w_s$ [mm] | $S$ [mm] | $h_s$ [mm] | $F_{max}$ [kN] | $f_{mean}$ [N.mm$^{-2}$] | 3DCP $f_{xk}$ [N.mm$^{-2}$] | Brick $f_{xk}$ [N.mm$^{-2}$] | Procentage |
|---|---|---|---|---|---|---|---|---|
| 4_211026-19 | 790 | 700 | 340 | 87.88 | 1.01 | 0.67 | 0.36 | 185% |
| 1_211026-20 | 790 | 700 | 340 | 67.27 | 0.77 | 0.52 | | 140% |
| 6_121026-21 | 790 | 700 | 340 | 99.75 | 1.15 | 0.76 | | 210% |
| 5_121026-22 | 790 | 700 | 340 | 96.60 | 1.11 | 0.74 | | 200% |
| 3_With steel | 780 | 700 | 335 | 22.26 | 0.27 | 0.18 | | 45% |
| 2_Without steel | 780 | 700 | 335 | 20.29 | 0.24 | 0.16 | | 40% |

where $w_s$ [mm] is wight of specimen, $f_{mean}$ [N.mm$^{-2}$] is the average bending strength.

## 4 Conclusion

Measurements were made on 3DCP wall segments made by ICE Industrial Services a.s. The testing was performed in the AdMaS centre where the test stand was set up. The load was applied perpendicular to the wall plane. Constant loading was performed by a hydraulic press. The segment loading was set at 1MPa.

Experimental measurements showed that the internal reinforcing columns have a great influence on the maximum load of the test elements. When loaded, wall segments without internal reinforcing columns show up to four times lower strength than reinforced columns.

Wall segments without internal reinforcing columns were created with the same geometry. The internal reinforcement of the structure is formed by the internal reinforcement of one of the columns, which makes them different from each other. This fact is reflected in the deformation of the wall. The specimen with the reinforcement has a higher deflection in the tensile region. The maximum force applied to the segment was determined by percentage difference with a value of 10%.

The test specimens with internal reinforcement columns, behave very similarly in failure. The results were compared according to round and square internal reinforcing columns. The two variants were divided according to the reinforcement. The segments with round columns were judged to be within 5% difference in maximum load when comparing the reinforcement variation. The square reinforcing columns were judged to be within 25% percentage difference when the same assessment was made. All percentage values were based on one measurement. Multiple test bodies need to be tested for stronger static value and probability.

This paper was written with the financial support of specific university research project FAST VUT, FAST-S-23-8413 (Data support for the design of green facades and roofs with integrated photovoltaic panels) and FAST-J-23-8344 (Investigation of the characteristic behaviour of reinforced elements and structures made by additive technology using a 3D concrete frame printer).

## References

1. I. Hager, A. Golonka, R. Putanowicz. Proc. Engi. **151**, 292-299 (2016)
2. J. Lluch-Cerezo, R. Benavente, M.D. Meseguer, S.C. Gutiérrez. Proc. Manu. **41**, 890-897 (2019)
3. E. Yasa, J. Deckers, J. Kruth. Rap. Prot. Jour. **11**, 312-327 (2011)
4. B. Dermeik, N. Travitzky. Adva. Engi. Mate. **22**, 24 (2020)
5. F. Hu, T. Mikolajczyk, D.Y. Pimenov, M.K. Gupta. Mate. **14**, 22 (2021)
6. I. Aydin, F.R. Biglari, B.J. Briscoe, C.J. Lawrence, M.J. Adams. Comp. Mate. Scie. **18**, 141-155 (2000)
7. S. Lim, R. Buswell, T. Le, R. Wackrow, S. Austin, A. Gibb, T. Thorpe. Proc. o. t. 28 ISA. 665-670 (2011)
8. A. Kazemian, X. Yuan, R. Meier, E. Cochran, B. Khoshnevis. Addi. Manu. **2**, 5 (2017)
9. T.T. Le, S.A. Austin, S. Lim, R.A. Buswell, A.G.F. Gibb, T. Thorpe. Mate. A. Struc. **45**, 1221-1232 (2012)
10. S. Huang, W. Xu, Y. Li, Fron. o. Arch. Rese. **11**, 653-669 (2022)
11. T.A.M. Salet, Z.Y. Ahmed, F.P. Bos, H.L.M. Laagland. Virt. a. Phys. Prot. **13**, 222-236 (2018)